Aga, Katsuaki; Hirata, Akimasa; Laakso, Ilkka; Tarao, Hiroo; Diao, Yinliang; Ito, Takahiro; Sekiba, Yoichi; Yamazaki, Kenichi

Intercomparison of in Situ Electric Fields in Human Models Exposed to Spatially Uniform Magnetic Fields

Published in:
IEEE Access

DOI:
10.1109/ACCESS.2018.2881277

Published: 01/01/2018

Document Version
Publisher's PDF, also known as Version of record

IEEE Access
Multidisciplinary | Rapid Review | Open Access Journal

Received October 17, 2018, accepted November 8, 2018, date of publication November 16, 2018,
date of current version December 18, 2018.

Digital Object Identifier 10.1109/ACCESS.2018.2881277

Intercomparison of *In Situ* Electric Fields in Human Models Exposed to Spatially Uniform Magnetic Fields

KATSUAKI AGA[1], AKIMASA HIRATA[1], (Fellow, IEEE), ILKKA LAAKSO[2], (Member, IEEE), HIROO TARAO[3], YINLIANG DIAO[4], (Member, IEEE), TAKAHIRO ITO[1], (Member, IEEE), YOICHI SEKIBA[5], AND KENICHI YAMAZAKI[6], (Senior Member, IEEE)

[1]Department of Electrical and Mechanical Engineering, Nagoya Institute of Technology, Nagoya 466-8555, Japan
[2]Department of Electrical Engineering and Automation, Aalto University, 02150 Espoo, Finland
[3]Department of Electrical and Computer Engineering, National Institute of Technology, Kagawa College, Takamatsu 761-8058, Japan
[4]College of Electronic Engineering, South China Agricultural University, Guangzhou 510642, China
[5]Denryoku Computing Center, Ltd., Tokyo 101-0054, Japan
[6]Central Research Institute of Electric Power Industry, Yokosuka 240-0196, Japan

Corresponding authors: Akimasa Hirata (ahirata@nitech.ac.jp) and Kenichi Yamazaki (yamazaki@criepi.denken.or.jp)

This work was supported by the Ministry of Internal Affairs and Communications, Japan (KA, AH, and TI).

ABSTRACT IEEE C95.1 (radio frequency) and C95.6 (low frequency) standards for human protection from electromagnetic fields are currently under revision. In the next revision, they will be combined into one standard covering the frequency range from 0 Hz to 300 GHz. Although the C95.1 standard considers anatomical human models for deriving the relationship between internal and external field strengths, homogeneous ellipses are used in the C95.6 standard. In the guidelines of the International Commission on Non-Ionizing Radiation Protection, anatomical human models are used together with reduction factors to account for numerical uncertainty. It is worth revisiting their relationship when using different anatomical models. In this paper, five research groups performed a comparative study to update the state-of-the-art knowledge of in situ electric fields in anatomical human models when exposed to uniform low-frequency magnetic fields. The main goals were to clarify both numerical uncertainty and model variability. The computational results suggest a high consistency among in situ field strengths across laboratories; agreement in the 99th percentile with a discrepancy of under 5% was achieved. The in situ electric fields varied as expected given the models' different dimensions. The induction factor, which is the ratio of the in situ electric fields for the temporal derivative of the external magnetic flux density, is derived for body parts and tissues. The classification of body parts into ''the limb'' and ''other tissues'' is shown to be critical for determining the in situ field strength.

INDEX TERMS Anatomical human models, human safety, dosimetry, magnetic fields, standardization.

I. INTRODUCTION

There has been public concern regarding potential adverse health effects of human exposure to electromagnetic fields. The World Health Organization (WHO) mentioned two international guidelines/standards of human protection from electromagnetic fields at low frequencies (LF), i.e., below 10 MHz: those issued by the International Commission on Non-Ionizing Radiation Protection (ICNIRP) and those by the IEEE (C95.6) [1], [2]. According to these guidelines/standards, the dominant effect associated with exposure to LF magnetic fields ($\sim$ 5 MHz [1] – 1 MHz [2]) is electrostimulation, which is caused by *in situ* electric fields.

Two different metrics are defined in these guidelines/standards. The first metric is the *in situ* (internal) electric field which is also called the basic restrictions or dosimetric reference limit [1], [2]. The main purpose of this study is to provide useful data for the revision of the IEEE standard. The other metric is the external electric/magnetic field strength, called as the reference level [2] or exposure reference level [1]. In the frequency range considered here, the *in situ* electric field is directly related to health effects or electrostimulation (pain or sensation). However, this is virtually impossible to measure practically. For this reason, the corresponding external field strength is defined for compliance purposes.

When deriving the relationship between external and internal field strengths, IEEE uses homogeneous ellipses with different dimensions for each body part whereas ICNIRP uses anatomical body models. The IEEE low-frequency standard will be revised in 2019 or later and the possibility of using anatomical body models has been discussed. The difference between the allowable external field strengths given by the ICNIRP guidelines and IEEE standard is a factor of 7–12.

One of the difficulties associated with using anatomical models as standards is the presence of numerical artifacts, which are inherent to voxelized models, which are created using a stair-casing approximation and discretization of the human body with a finite dimension of voxels [3]. The electromagnetic computation for an anatomical model does not have exact solution, making proper comparison complicated.

The ICNIRP guidelines applied an additional reduction factor of 3 when deriving the reference level from the basic restriction. Even though the 99th percentile value is specified by ICNIRP to exclude singularities, international experts continue to discuss its effectiveness for exploring better metrics (e.g., [4]–[8]).

The research agenda of IEEE ICES (International Committee on Electromagnetic Safety) highlights the necessity of resolving numerical issues [9] It also states that *"It would be helpful to compare the induction factors applicable to different physical representations of the human body, as well as for the same body model as encoded into computational models by different organizations."* Note that the induction factor here is defined as the ratio of *in situ* electric fields for the temporal derivative of the external magnetic flux density. Even though the IEEE standard classifies the brain, heart, and other tissues for human protection, until now, no comparative study has been conducted to evaluate these metrics Computational techniques using anatomical body models have been developed (e.g., [10]–[15]) following a comparative study conducted 10 years ago [16] (see Sec. II)

The purpose of the present study is to conduct the intercomparison of the *in situ* electric field in different body parts prescribed by the IEEE standard using different human body models. The induction factors for different tissues/organs prescribed in the IEEE standard are then derived for different models to provide essential metrics for setting the limit in future revisions of the standard

II. REVIEW OF COMPUTATIONAL DOSIMETRIC STUDIES FOR STANDARDIZATION

The first intercomparison and review on LF magnetic field exposure was published in [17]. In the 1990s, computations using numerical human models were conducted at the University of Utah [18] and at the University of Victoria [19]. The resolutions of the two models were 7.2 mm and 6 mm, respectively, which are insufficient to represent the average-strength *in situ* electric field prescribed by the international guidelines/standards. Different conductivities were used due to the lack of reliable databases at the time. The groups then conducted an intercomparison of *in situ* electric fields and current densities with those reported by the National Radiological Protection Board [20]. The relative difference was a factor of 2 at most.

In the following years, different anatomical models have been developed by different organizations. In addition, several groups have independently developed computational codes for LF dosimetry. An intercomparison study was coordinated by a technical committee of the IEE Japan using a standard Japanese model [16]. This study used an extensive database and, unlike the earlier intercomparison, identical sets of electrical conductivities and exposure conditions were used. The differences between the results obtained by the different participating groups were generally under 10–20%, excluding singular results. In that study, only one anatomical model was considered.

A few research groups discussed additional numerical issues including skin-to-skin contact [21]–[23]; further computational uncertainty was discussed. Several researchers have also developed unique codes with the goal of improving product safety or compliance (e.g. [10]–[15], [24]–[26]). In [12], the computed *in situ* electric field at the allowable external field strength was calculated to exceed the allowable *in situ* electric field in one model. Thus, the metrics used in these studies may not match or satisfy the data requirements needed to revise the IEEE standard. Nagoya Institute of Technology (NITech) and Aalto University conducted preliminary computations for setting the conditions for the intercomparison, including the classification of trunk/limbs, where different limits should be applied according to the current version of the IEEE C95.6 standard [21].

III. MODEL AND METHODS

A. HUMAN BODY MODELS

We considered six different human models, as shown in Fig. 1. Models a, b) are Japanese male and female adults, named TARO and HANAKO, that were developed by the National Institute of Information and Communications Technology (NICT) [27]; c, d) European male and female models, named Duke and Ella, that were developed by the IT'IS Foundation [28]; e) the standardized model, NORMAN, developed by the National Radiological Protection Board [20];

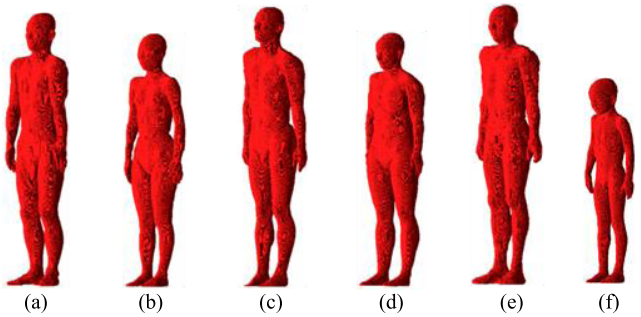

FIGURE 1. Anatomical human body models: (a) TARO, (b) HANAKO, (c) Duke, (d) Ella, (e) NORMAN, (f) Thelonious.

TABLE 1. Characteristics of the six anatomical body models.

Name	Height [m]	Weight [kg]	Number of Tissues
(a) TARO	1.73	65	51
(b) HANAKO	1.61	53	51
(c) Duke	1.74	70	77
(d) Ella	1.60	58	74
(e) NORMAN	1.76	73	37
(f) Thelonious	1.17	20	73

and f) the child model, named Thelonious, that was developed by the IT'IS Foundation [28]. Duke version 1 was used for intercomparison to assess the fundamental numerical uncertainty. Note that version 1 was used due to licensing issues.

The models are based on magnetic resonance images and are composed of more than 50 tissues and organs, such as skin, muscle, bone, and so on. Table 1 summarizes the main characteristics of the six anatomical body models. The original model resolutions varied. For example, some models were scalable to the desired resolution. We set the desired model resolution as 2 mm $\times$ 2 mm $\times$ 2 mm, which is the original resolution of TARO and HANAKO models.

In the IEEE C95.6 standard, a basic restriction was specified for four types of tissues/organs: brain, heart, limbs, and other tissues (which includes peripheral nerves). Therefore, the blue area of the anatomical models shown in Fig. 2 corresponding to the arms and legs, was defined as the limbs. The human body tissues except for the brain, heart, and limbs are categorized as ''other tissues'' Even though no detailed classification is given in the IEEE C95.6 standard, the definitions used in this intercomparison are shown in Fig. 2. Without any adjustments, a difference of $\sim$40% was observed in the preliminary assessment of *in situ* electric fields [29].

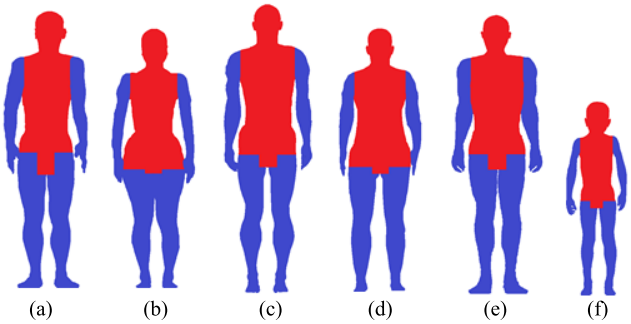

FIGURE 2. Classification of limbs in the different anatomical human body models: (a) TARO, (b) HANAKO, (c) Duke, (d) Ella, (e) NORMAN, (f) Thelonious.

B. TISSUE CONDUCTIVITIES

Table 2 shows the tissue electrical conductivities used in the present study. These values were determined based on the report in [30]. The effect of tissue permittivity on *in situ* quantities in the LF region was marginal because the conduction current was dominant compared with the displacement current [31], [32]. Thus, the tissue permittivity was ignored in our computation. The skin conductivity was set to 0.10 S/m and 0.50 S/m for frequencies up to 3 kHz and at 1 MHz, respectively, based on the discussion in [22] and [33]. In addition, the dielectric properties reported in [34] were used to consider the effect of conductivity on *in situ* electric fields. The parameters were based on the Gabriel dispersion relationships [23]. However, the dielectric properties for some tissues are not well-documented. In these cases, the properties of a similar anatomical organization were used as an approximation. For example, the properties of the mandible, patella and vertebrae bones were substituted by those of cortical bone. Also, several lumens in the IT'IS models were replaced by air with no conductivity. Note that the influence on the *in situ* electric field is extremely small because the tissues occupying most of the human body structure were not changed.

TABLE 2. Conductivity of human tissues at 50 Hz and 1 MHz as determined by Gabriel (1996) [S/m].

Tissues	50 Hz	1 MHz	Tissues	50 Hz	1 MHz
Skin	0.10	0.50	Pancreas	0.52	0.58
Muscle	0.23	0.50	Spleen	0.09	0.18
Fat	0.04	0.04	Stomach	0.52	0.58
Cartilage	0.17	0.23	Bile	1.40	1.40
Nerve	0.03	0.13	Lymph	0.52	0.60
Bone marrow	0.10	0.10	Glands	0.52	0.60
Gray matter	0.08	0.16	Bladder	0.21	0.24
White matter	0.05	0.10	Testicles	0.42	0.56
Cerebellum	0.10	0.19	Tooth	0.02	0.02
CSF	2.00	2.00	Gall bladder	0.90	0.90
Vitreous humor	1.50	1.50	Nails	0.02	0.02
Cornea	0.42	0.66	Dura	0.50	0.50
Lens	0.32	0.37	Tongue	0.27	0.39
Sclera	0.50	0.62	Skull	0.05	0.06
Heart	0.08	0.33	Trachea	0.30	0.37
Liver	0.04	0.19	Esophagus	0.52	0.58
Lung	0.07	0.14	Tendon	0.27	0.39
Kidneys	0.09	0.28	Iris	0.50	0.62
Small intestine	0.52	0.86	Breast	0.02	0.03
Colon	0.05	0.31	Ovary	0.32	0.36
Blood	0.70	0.82	Uterus	0.23	0.56
Blood vessel	0.26	0.33	Duodenum	0.52	0.58
Bone (Cortical)	0.02	0.02	Testis prostate	0.42	0.56
Bone (Cancellous)	0.08	0.09	Anterior chamber	1.50	1.50
Mucous membrane	0.00	0.22	Thyroid thymus	0.52	0.60

C. COMPUTATIONAL METHODS

Magneto-quasi-static approximation is valid in the frequency range considered here. In this frequency range, the electromagnetic fields can be decoupled into the magnetic field and electric field components. In this study, the exposure to the magnetic field is considered because these scenarios are more common in daily life except directly under power lines.

There are several computational methods used for electromagnetic dosimetry in the magneto-quasi-static regime [35]: scalar potential finite difference (SPFD) [31], voxel-based finite element method (FEM), impedance [36], quasi-static finite-difference time-domain (FDTD) [37] etc. The impedance method was not considered here because the electric field (vector component) is used in the computation meaning its computational cost is approximately 10 times greater than that of the SPFD method (see [20]). The quasi-static FDTD method was not considered because, unlike other quasi-static method, it does not handle computational error easily because it has no criteria for numerical convergence.

The SPFD method [31] was used at NITech, South China Agricultural University (SCAU), and Central Research Institute of Electric Power Industry (CRIEPI).

The SPFD method sets the branch current instead of the eddy current. Defining scalar potentials (unknowns) at each node of a voxel, a branch current flowing from one node to a neighboring one along the side of a voxel is derived, which includes the vector potential owing to the applied magnetic field and the impedance mismatch between the nodes.

$$\sum_{n=1}^{6} S_n \varphi_n - \left(\sum_{n=1}^{6} S_n\right) \varphi_0 = j\omega \sum_{n=1}^{6} (-1)^n S_n l_n A_{0n}, \quad (1)$$

In Eq. (1), S_n, ϕ_n, l_n, ω, and A_{0n} denote the edge conductance derived from the tissue conductivity, the scalar potential, the length between the nodes, the angular frequency, and the magnetic vector potential, respectively. Kagawa College also uses the SPFD method, but the scalar potentials are defined at the center of each voxel, although the governing equation is the same.

Applying Kirchhoff's current law to all nodes, simultaneous equations are obtained. The electric field along the side of a voxel is obtained by dividing the potential difference between the nodes of the voxel by the distance across the nodes, and then adding the vector potential.

$$\mathbf{E} = -\nabla\varphi_0 - j\omega\mathbf{A_0}, \quad (2)$$

A finite element method (FEM) [38] with first-order cubical elements was used at Aalto University. Under the quasi-static assumption, the electric field can be represented as

$$\mathbf{E} = -\nabla\varphi - \frac{\partial}{\partial t}\mathbf{A_0}, \quad (3)$$

where φ is the electric scalar potential and $\mathbf{A_0}$ is the vector potential of the incident magnetic field. Because of the continuity condition, the electric scalar potential satisfies the following elliptic partial differential equation

$$\nabla \cdot \sigma\nabla\varphi = -\nabla \cdot \sigma\frac{\partial}{\partial t}\mathbf{A_0}, \quad (4)$$

with the boundary condition

$$\mathbf{n} \cdot (\nabla\varphi + \frac{\partial}{\partial t}\mathbf{A_0}) = 0, \quad (5)$$

The matrix equations for the SPFD method at NITech and for the FEM at Aalto University were solved iteratively using the geometric multigrid method with successive over-relaxation smoothing [39]. The conjugate gradient method with incomplete Cholesky preconditioner (Kagawa College) [40], the bi-conjugate gradient stabilized method (CRIEPI) [41], and the Jacobi iterative method (SCAU) [42] were used as well.

Previous studies determined that a sufficient stopping criterion to allow a truncation error of 1% for non-uniform exposure is on the order of 10^{-5} in terms of the relative residual [39]. In this study similarly, the criterion for uniform exposure was a relative residual of 10^{-6}. Thus, the relative residual of 10^{-6} was used in all organizations for proper comparison.

D. CONFIRMATION OF OUR COMPUTATIONAL CODES AND DEFINITION OF RELATIVE DIFFERENCE

No exact solution exists for electromagnetic analysis of the anatomical models. The above-mentioned computational code has been confirmed by comparing the induced field in a multi-layer sphere. The computational error of the 99$^{\text{th}}$ percentile value of the*in situ* electric field was largest at the outer layer (skin) and less than 10% using each of the codes. Note that due to the stair-casing error the maximum *in situ* electric field is larger than the analytic solution. The error in the brain was less than a few percent, which is consistent with previous findings [5], [43]

For intercomparison of results by different groups, a reference value, A_r, was introduced. It is the mean of the results obtained by the five research groups. This definition is necessary because of the lack of the exact solution of anatomical models. The relative difference D between the reference value and the results calculated by either one of the groups is defined by the following expression:

$$D = \frac{A_i - A_r}{A_r}, \quad (6)$$

where the subscripts r and i correspond to the data for the reference value and that obtained by the i-th group, respectively

E. EXPOSURE SCENARIOS AND EVALUATION METRICS

A human model was placed in free space with a standing posture. We conducted dosimetry for six anatomical body models in the coronal direction (AP) exposure, in which the *in situ* (induced) electric field is maximal [1]. With respect to the strength of the external uniform magnetic field, the magnetic flux density was 0.1 mT and the frequencies were 50 Hz and 1 MHz, respectively, for computational uncertainty analysis. In the ICNIRP guideline, the reference level of the magnetic field is determined assuming a uniform magnetic field. Also, these frequencies are close to lower- (1 Hz) and higher-limit frequencies (5 MHz) [1]. For assessing the variability across the different models, the frequencies of 50 Hz, 759 Hz, 1 kHz, 3 kHz, and 1 MHz were chosen. The frequency of 759 Hz was chosen accounting for the transition frequency

of the maximal permissible exposure in the IEEE C95.6 standard [1]. Note that different limits are prescribed for different tissues. The threshold of the tissue depends on variables like nerve fiber diameters. These differences are considered while defining the relationship between internal and external field strengths.

The *in situ* electric fields corresponding to ellipsoidal induction models in the IEEE C95.6 standard for magnetic field exposure at 0.1 mT, at the frequencies of 50 Hz and 1 MHz, are listed in Table 3. These values are defined by the following equation [1]:

$$E = \omega B \frac{\sqrt{a^4u^2 + b^4v^2}}{a^2 + b^2}, \tag{7}$$

where ω and B are the angular frequency and the magnetic flux density, respectively, a and b are the semi-major and semi-minor axes, respectively, and u and v capture the location within the exposed area. To define the allowable values for the four types of tissues/organs (brain, heart, limbs, and other tissues), ω and B were used for the above conditions, and other parameters were listed in [1]. An exposure scenario for whole-body uniform magnetic field is considered although the IEEE standard assumes exposure conditions for individual body parts.

TABLE 3. ***In Situ*** **electric field for magnetic field exposure at 0.1 mT, calculated using the ellipsoidal magnetic induction model of the IEEE C95.6 standard.**

Exposed Tissue	50 Hz [mV/m]	1 MHz [V/m]
Brain	1.63	32.6
Heart	4.25	85.0
Limbs	2.70	54.1
Other tissues	5.16	103

The averaging metrics used by the standardization bodies differ; IEEE uses the *in situ* (or induced) electric field averaged over a straightline segment of 5 mm [1] while ICNIRP uses an average over a 2 mm cube [2]. In the latter, the 99th percentile value [2] should also be used considering the numerical artifacts that are inherent in LF computation with voxel human models.

In this study, the 99th percentile value was used as the maximal value of the *in situ* electric field for simplicity. The skin-to-skin contact regions with stair-casing error are mostly excluded in post-processing. Note that while the IEEE uses the *in situ* electric field averaged over a straightline segment of 5 mm [1] this is not used here because the goal of the present work is to clarify the numerical uncertainty in the intercomparison. The difference in the electric fields calculated using a 2-mm cube and 5 mm straight line was, however, on the order of 20–30% for the skin [44]. The difference of the threshold *in situ* electric field in IEEE and ICNIRP for brain tissue stimulation was 5% [45].

IV. COMPUTATIONAL RESULTS AND DISCUSSION

A. COMPUTATIONAL VARIATION OF THE IN SITU ELECTRIC FIELD IN THE ANATOMICAL BODY MODELS

In situ electric fields at 50 Hz for the TARO, HANAKO, and Duke models are shown in Fig. 3 (a)–(c), respectively. As shown in Fig. 3 (a)–(c), a small difference is observed, especially in places of weird shapes, such as the neck and armpits. The reason is that *in situ* electric field is the greatest at certain places where the limbs and torso are connected, such as at the armpits, and the crotch. For all groups, only HANAKO demonstrated high *in situ* electric field in the legs (Fig. 3 (b)).

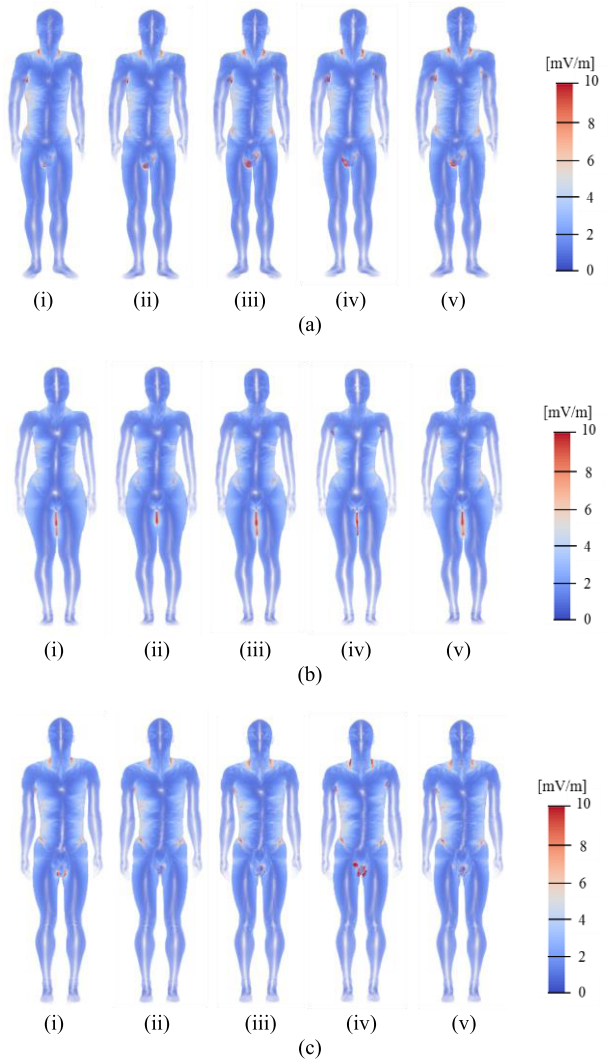

FIGURE 3. ***In situ*** **electric field distribution: (i) NITech, (ii) Kagawa, (iii) CRIEPI, (iv) Aalto Univ, (v) SCAU. Models: (a) TARO, (b) HANAKO, (c) Duke.**

Tables 4(a) and 4 (b) show the 99th percentile value for the*in situ* electric field, for different body regions and three different anatomical models, for the uniform magnetic field exposure at 50 Hz and 1 MHz, respectively.

TABLE 4. The 99th percentile values of the *in situ* electric field (*Ai*) for uniform magnetic field (0.1 mT) exposure at (a) 50 Hz and (b) 1 MHz. units: (a): mV/m, (b): V/m.

(a)

Exposed Tissue	NITech			Kagawa			CRIEPI			Aalto			SCAU		
	TARO	HANAKO	Duke	TARO	HANAKO	Duke	TARO	HANAKO	Duke	TARO	HANAKO	Duke	TARO	HANAKO	Duke
Brain	2.62	2.50	2.50	2.22	2.03	2.11	2.61	2.48	2.46	2.71	2.59	2.50	2.61	2.48	2.47
Heart	3.73	2.41	3.24	3.69	2.27	3.18	3.59	2.46	3.37	3.59	2.38	3.80	3.53	2.45	3.68
Limbs	3.04	5.43	2.65	2.99	4.27	2.65	3.11	7.09	2.78	2.94	3.40	2.70	3.10	7.10	2.79
Others	6.08	5.07	6.27	6.08	5.01	6.51	6.99	5.46	7.39	5.78	4.92	6.50	6.99	5.46	7.34

(b)

Exposed Tissue	NITech			Kagawa			CRIEPI			Aalto			SCAU		
	TARO	HANAKO	Duke	TARO	HANAKO	Duke	TARO	HANAKO	Duke	TARO	HANAKO	Duke	TARO	HANAKO	Duke
Brain	44.9	42.2	43.2	38.7	36.3	38.1	44.9	41.9	42.4	45.1	42.6	43.4	44.9	41.9	42.7
Heart	47.9	37.3	54.5	46.4	37.1	51.4	47.1	37.6	52.2	48.4	37.2	53.0	47.0	37.5	53.2
Limbs	64.0	145	57.1	63.0	106	57.2	66.9	175	60.6	64.7	157	57.0	66.7	176	60.6
Others	140	111	141	146	114	150	161	123	163	131	107	141	161	123	162

TABLE 5. Averaged values (*Ar*) and relative differences (*D*) of the 99th percentile values of the *in situ* electric field for uniform magnetic field (0.1mT) exposure at 50 Hz(a), (c), (e) and at 1 MHz(b), (d), (f). Models: (a), (b): TARO, (c), (d): HANAKO, (e),(f): Duke.

(a)

Exposed tissue	Average [mV/m]	Relative difference [%]				
		NITech	Kagawa	CRIEPI	Aalto	SCAU
Brain	2.55	2.43	-12.9	2.08	6.27	2.13
Heart	3.63	2.91	1.73	-0.99	-0.96	-2.69
Limbs	3.04	0.10	-1.49	2.52	-3.06	1.93
Others	6.38	-4.68	-4.72	9.44	-9.50	9.45

(b)

Exposed tissue	Average [V/m]	Relative difference [%]				
		NITech	Kagawa	CRIEPI	Aalto	SCAU
Brain	43.7	2.85	-11.4	2.71	3.14	2.71
Heart	47.4	1.18	-2.06	-0.48	2.14	-0.79
Limbs	65.1	-1.65	-3.21	2.76	-0.48	2.59
Others	148	-5.14	-1.52	8.94	-11.3	8.99

(c)

Exposed tissue	Average [mV/m]	Relative difference [%]				
		NITech	Kagawa	CRIEPI	Aalto	SCAU
Brain	2.42	3.58	-16.2	2.64	7.31	2.66
Heart	2.39	0.56	-5.14	2.83	-0.80	2.54
Limbs	5.46	-0.49	-21.7	29.9	-37.7	30.1
Others	5.18	-2.22	-3.32	5.29	-5.03	5.28

(d)

Exposed tissue	Average [V/m]	Relative difference [%]				
		NITech	Kagawa	CRIEPI	Aalto	SCAU
Brain	41.0	2.95	-11.5	2.21	4.07	2.25
Heart	37.3	0.02	-0.74	0.58	-0.28	0.42
Limbs	152	-4.39	-30.4	15.6	3.44	15.8
Others	116	-4.34	-1.32	6.67	-7.69	6.67

(e)

Exposed tissue	Average [mV/m]	Relative difference [%]				
		NITech	Kagawa	CRIEPI	Aalto	SCAU
Brain	2.41	3.88	-12.5	2.20	3.90	2.48
Heart	3.45	-6.27	-7.88	-2.43	10.0	6.58
Limbs	2.71	-2.43	-2.32	2.47	-0.52	2.80
Others	6.80	-7.78	-4.34	8.70	-4.44	7.86

(f)

Exposed tissue	Average [V/m]	Relative difference [%]				
		NITech	Kagawa	CRIEPI	Aalto	SCAU
Brain	42.0	3.03	-9.19	1.10	3.37	1.69
Heart	52.9	3.08	-2.81	-1.22	0.24	0.72
Limbs	58.5	-2.33	-2.18	3.51	-2.58	3.59
Others	151	-6.63	-1.01	7.54	-7.02	7.12

To analyze the results obtained by different groups, the relative difference D for the 99th percentile values of the *in situ* electric field is listed in the Table 5.

For the TARO model, the maximal relative difference was 12.9%, which appeared for the brain computed by Kagawa College. The other difference larger than 10% was observed in other tissues, computed by Aalto University. These differences might be attributed to differences between the computational methods. Indeed, in the study by Kagawa College nodes were defined differently in the SPFD, compared with the FEM that was used at Aalto University.

A similar tendency was observed also for the HANAKO model, except for the limbs, where a more significant difference was observed between the *in situ* fields of the models' limbs compared with that reported by the other two models. This difference arises because the legs in the HANAKO model are in contact each other making a larger loop for the fields to be induced [21]–[23]. For HANAKO, the electric field in the limbs was twofold higher than that for the other two models.

The tendency observed in TARO was also seen in Duke. The maximal relative difference was 12.5%, which corresponded to the brain computed by the group at Kagawa College and is similar to that found by other models This confirmed that the results of the calculations by the five research groups were in a good agreement with a mean relative difference of 4.3% and maximal relative difference of 16.2% (excluding the limbs of HANAKO)

TABLE 6. Comparison of the *in situ* electric field for duke, for different sets of dielectric properties: (a) 50 Hz and (b) 1 MHz.

(a)

Exposed tissue	*In situ* electric field [mV/m] Gabriel	IT'IS	Average	Relative difference [%]
Brain	2.50	2.49	2.50	0.10
Heart	3.24	3.53	3.38	-4.27
Limbs	2.65	2.65	2.65	-0.11
Others	6.27	6.32	6.29	-0.34

(b)

Exposed tissue	*In situ* electric field [V/m] Gabriel	IT'IS	Average	Relative difference [%]
Brain	43.2	43.2	43.2	0.04
Heart	54.5	47.6	51.0	6.77
Limbs	57.1	57.2	57.2	-0.03
Others	141	143	142	-0.53

TABLE 7. Mean of the 99th percentile values of The *in situ* electric field [mV/m], computed at NITech and Aalto university. The column labeled IEEE C95.6 corresponds to the ellipsoidal induction model. (50 Hz and 1 MHz results shown in table 4).

Exposed Tissue	Frequency [Hz]	IEEE C95.6	TARO	HANAKO	Duke	Ella	NORMAN	Thelonious
Brain	50	1.63	2.66	2.55	2.50	2.13	2.93	2.08
	759	24.7	38.5	36.9	36.7	31.3	42.5	30.5
	1,000	32.6	50.6	48.4	48.3	41.2	55.9	40.2
	3,000	97.8	150	143	143	123	165	119
	1,000,000	32600	45000	42400	43300	38400	49500	37400
Heart	50	4.25	3.66	2.39	3.52	2.06	3.70	1.29
	759	64.5	52.8	34.6	52.7	29.8	50.4	19.8
	1,000	85.0	68.9	45.1	68.8	39.0	65.8	26.0
	3,000	255	192	127	196	109	183	75.9
	1,000,000	85000	48200	37300	52800	32400	48800	23800
Limbs	50	2.70	2.99	4.42	2.67	2.80	3.12	1.74
	759	41.0	47.1	96.7	41.4	44.6	55.9	26.7
	1,000	54.1	62.1	128	54.6	58.8	73.7	35.1
	3,000	162	186	385	164	176	221	105
	1,000,000	54100	64400	151000	57100	65100	79600	37600
Others	50	5.16	5.93	5.00	6.39	5.67	7.23	3.64
	759	78.3	95.3	79.1	102	87.9	117	57.9
	1,000	103	126	104	134	116	154	76.4
	3,000	309	380	314	404	348	466	229
	1,000,000	103000	136000	109000	141000	119000	166000	74600

B. VARIABILITY OF THE IN SITU ELECTRIC FIELD ACROSS DIFFERENT CONDUCTIVITY VALUES

The effect of tissue conductivity on the *in situ* electric field was investigated using the Duke model and the code provided by NITech. In addition to the set of dielectric properties compiled by Gabriel, the set of parameter values compiled by the IT'IS foundation was used, and the results obtained using these two parameter sets are listed in Table 6. Note that the conductivity of the skin was the same as discussed above. As shown in Table 6, the relative difference excluding the heart was smaller than 1.0%, suggesting that for used dielectric parameters, the effect of the conductivity is marginal. Note that the dielectric properties of major tissues, such as muscle and fat, are identical across the two data sets. The *in situ* electric field in the heart is relatively easily influenced by the effect of the conductivity This effect is attributable to the relatively high and low conductivities of the surrounding structures, blood and lumens

C. VARIABILITY OF IN SITU ELECTRIC FIELD ACROSS DIFFERENT BODY MODELS

To assess the variability of the *in situ* electric field across different human models, we considered the six anatomical models: TARO, HANAKO, Duke, Ella, NORMAN, and Thelonious. The mean values of the *in situ* electric fields computed at NITech and Aalto University were used. Note that the average value of the relative difference between these two groups was 5.6%; excluding the limbs of HANAKO, it was 4.9%. Table 7 shows the average value of the *in situ* electric field for different body parts and different frequencies. The frequencies were chosen so as to cover the frequencies up to the maximal permissible exposure in the IEEE C95.6 standard.

As shown in Table 7, NORMAN in general exhibited the maximal values, except for the heart. By Faraday's law, this can be attributed at least partially to the fact that NORMAN is larger than the other models (Table 1). Comparable results were observed for adult male models TARO and Duke. The *in situ* electric field was smallest for Thelonious (the child model).

The *in situ* electric field in the heart was strongest for TARO (except at 3 kHz and 1 MHz). This discrepancy arises because the heart is an internal organ; thus, the induction current in the heart is affected by the surrounding anatomy. This explains why the variability across the models was relatively large for the heart (Fig. 3). The variability in the limb was large because of skin-to-skin contact, as mentioned in the previous section.

Table 8 lists the ratio of the *in situ* electric field (maximal value across all the models, excluding limbs in HANAKO) to the allowable field strength derived from the

TABLE 8. Ratio of The maximum magnetic field coupling for each tissue and frequency shown in table 7 to the corresponding coupling for the ellipsoid in IEEE C95.6.

Frequency [Hz]	Brain	Heart	Limbs	Others
50	1.80	0.87	1.16	1.40
759	1.72	0.82	1.36	1.49
1,000	1.72	0.81	1.36	1.50
3,000	1.69	0.77	1.36	1.51
1,000,000	1.52	0.63	1.47	1.61

* Excludes limbs for HANAKO

IEEE C95.6 ellipsoidal induction model for each part. As shown in Table 8, the *in situ* electric field intensity ratio exceeds the unity by 80% for the brain and by 15–60% for the limb and other tissues. This underestimation arises because an isolated and homogeneous ellipsoidal model was considered in the C95.6 standard calculation. Instead, as shown in Fig. 3, the peak *in situ* electric field intensity appeared at the place where the structure was complicated and/or the tissue boundary was obvious, as discussed in previous studies. The field strength in the brain is underestimated because the effect of the isolated model is significant; based on Faraday's law, the current induced in the brain is large.

V. CONCLUSION

Intercomparison of the *in situ* electric field distributions for low-frequency magnetic field exposure was coordinated under the editorial working group #2 of IEEE ICES in conjunction with subcommittee 6. The numerical uncertainty caused by the use of different codes was ∼5%, assuming the same conditions. This uncertainty was gradually reduced using advances in computational techniques; it was 200% in 2000 [17] and 10% or more in 2010 [16]. An additional difference may arise when interpolation or additional post-processing is applied [7]. However, the uncertainty is emphasized when the skin-to-skin contact exists, as in the model HANAKO. This issue has been discussed extensively elsewhere; however, when considering the anisotropy of skin layers and a finite resolution of the anatomical model, this issue is not crucial when deriving the relationship between the *in situ* and external field strengths. If such computational modeling is directly used for development of product safety and/or compliance guidelines, further attention would be required to properly treat this issue. Variability in the models were caused by the differences in their cross-sectional areas, as expected by the ellipses in the IEEE C95.6 standard and Faraday's law.

Computational results for the *in situ* electric field in the brain, limbs, and other tissues were then higher than the values obtained using the ellipsoidal induction model. This implies that, even if the reference level of the magnetic field is satisfied, the basic restriction may not always be satisfied in the IEEE standard. This follows from the fact that the MPEs of IEEE C95.6 were directly derived from the basic restrictions using the isolated and homogeneous ellipsoidal model. For example, for the brain, the remaining part and anatomy of the head may influence the *in situ* field strength. The induction factors obtained here would be useful for relating the internal and external field strengths for uniform exposures. Some exceedance of the factor from the ellipse should be discussed as a replacement for the reduction factor in the existing guidelines/standards.

In future work, we will further explore metrics that are more stable than the 99th percentile for uniform exposure, which may provide an improved estimate of the maximum dose. In addition, there is a need to consider how to treat variances in the results obtained using standards based on anatomical models or ellipses. The difference for partial body (non-uniform) exposure from uniform exposures should also be discussed.

ACKNOWLEDGEMENTS

This study has been conducted as a task force under the editorial working group #2 of the IEEE International Committee of Electromagnetic Safety Technical Committee 95 in cooperation with subcommittee 6. The authors would like to thank members who supported this study, in particular Drs. Xi Lin Chen, Xiyao Xin, Xin Huan (Abbott Laboratories) for their discussion on the computational variability and members (J. Patrick Reilly, Robert Kavet, and Valerio De Santis) who reviewed the manuscript before submission.

REFERENCES

[1] *IEEE Standard for Safety Levels With Respect to Human Exposure to Electromagnetic Fields, 0 to 3 KHz*, IEEE Standard IEEE-C95.6, New York, NY, USA, 2002.

[2] International Commission on Non-Ionizing Radiation Protection, "Guidelines for limiting exposure to time-varying electric and magnetic fields (1 Hz to 100 kHz)," *Health Phys.*, vol. 99, no. 6, pp. 818–836, 2010.

[3] A. Hirata, K. Caputa, T. W. Dawson, and M. A. Stuchly, "Dosimetry in models of child and adult for low-frequency electric field," *IEEE Trans. Biomed. Eng.*, vol. 48, no. 9, pp. 1007–1012, Sep. 2001.

[4] B. Kos, B. Valič, D. Miklavčič, T. Kotnik, and P. Gajšek, "Pre- and post-natal exposure of children to EMF generated by domestic induction cookers," *Phys. Med. Biol.*, vol. 56, no. 19, p. 6149, 2011.

[5] I. Laakso and A. Hirata, "Reducing the staircasing error in computational dosimetry of low-frequency electromagnetic fields," *Phys. Med. Biol.*, vol. 57, no. 4, pp. N25–N34, 2012.

[6] D. Poljak *et al.*, "On the use of conformal models and methods in dosimetry for nonuniform field exposure," *IEEE Trans. Electromagn. Compat.*, vol. 60, no. 2, pp. 328–337, Apr. 2018.

[7] J. Gomez-Tames, I. Laakso, Y. Haba, A. Hirata, D. Poljak, and K. Yamazaki, "Computational artifacts of the *in situ* electric field in anatomical models exposed to low-frequency magnetic field," *IEEE Trans. Electromagn. Compat.*, vol. 60, no. 3, pp. 589–597, Jun. 2018.

[8] V. De Santis and X. L. Chen, "On the issues related to compliance assessment of ICNIRP 2010 basic restrictions," *J. Radiol. Protection*, vol. 34, no. 2, pp. N31–N39, 2014.

[9] J. P. Reilly and A. Hirata, "Low-frequency electrical dosimetry: Research agenda of the IEEE International Committee on Electromagnetic Safety," *Phys. Med. Biol.*, vol. 61, no. 12, p. R138, 2016.

[10] Y. L. Diao, W. N. Sun, Y. Q. He, S. W. Leung, and Y. M. Siu, "Equivalent magnetic vector potential model for low-frequency magnetic exposure assessment," *Phys. Med. Biol.*, vol. 62, no. 19, p. 7905, 2017.

[11] H. Tarao, H. Miyamoto, L. Korpinen, N. Hayashi, and K. Isaka, "Simple estimation of induced electric fields in nervous system tissues for human exposure to non-uniform electric fields at power frequency," *Phys. Med. Biol.*, vol. 61, no. 12, p. 4438, 2016.

[12] X.-L. Chen *et al.*, "Analysis of human brain exposure to low-frequency magnetic fields: A numerical assessment of spatially averaged electric fields and exposure limits," *Bioelectromagnetics*, vol. 34, no. 5, pp. 375–384, Jul. 2013.
[13] T. Shimamoto, I. Laakso, and A. Hirata, "*In-situ* electric field in human body model in different postures for wireless power transfer system in an electrical vehicle," *Phys. Med. Biol.*, vol. 60, no. 1, p. 163, 2014.
[14] A. Christ *et al.*, "Exposure of the human body to professional and domestic induction cooktops compared to the basic restrictions," *Bioelectromagnetics*, vol. 33, no. 8, pp. 695–705, 2012.
[15] H. Tarao, N. Hayashi, and K. Isaka, "Numerical analysis of induced current in human head exposed to nonuniform magnetic field including harmonics," *IEEJ Trans. Fundam. Mater.*, vol. 123, no. 11, pp. 1100–1107, 2003.
[16] A. Hirata *et al.*, "Intercomparison of induced fields in Japanese male model for ELF magnetic field exposures: Effect of different computational methods and codes," *Radiat. Protection Dosimetry*, vol. 138, no. 3, pp. 237–244, 2010.
[17] M. A. Stuchly and O. P. Gandhi, "Inter-laboratory comparison of numerical dosimetry for human exposure to 60 Hz electric and magnetic fields," *Bioelectromagnetics*, vol. 21, no. 3, pp. 167–174, 2000.
[18] O. P. Gandhi and J.-Y. Chen, "Numerical dosimetry at power-line frequencies using anatomically based models," *Bioelectromagnetics*, vol. 13, no. S1, pp. 43–60, 1992.
[19] T. W. Dawson and M. A. Stuchly, "High-resolution organ dosimetry for human exposure to low-frequency magnetic fields," *IEEE Trans. Magn.*, vol. 34, no. 3, pp. 708–718, May 1998.
[20] P. J. Dimbylow, "Induced current densities from low-frequency magnetic fields in a 2 mm resolution, anatomically realistic model of the body," *Phys. Med. Biol.*, vol. 43, no. 2, pp. 221–230, 1998.
[21] G. Schmid, S. Cecil, and R. Überbacher, "The role of skin conductivity in a low frequency exposure assessment for peripheral nerve tissue according to the ICNIRP 2010 guidelines," *Phys. Med. Biol.*, vol. 58, no. 13, pp. 4703–4716, 2013.
[22] V. De Santis, X. L. Chen, I. Laakso, and A. Hirata, "An equivalent skin conductivity model for low-frequency magnetic field dosimetry," *Biomed. Phys. Eng. Express*, vol. 1, no. 1, p. 015201, 2015.
[23] C. Li and T. Wu, "Dosimetry of infant exposure to power-frequency magnetic fields: Variation of 99th percentile induced electric field value by posture and skin-to-skin contact," *Bioelectromagnetics*, vol. 36, no. 3, pp. 204–218, 2015.
[24] S.-E. Hong, I.-K. Cho, J.-H. Kwon, and J.-K. Pack, "Assessment of human exposure to electromagnetic fields from wireless power transfer system in the 1.8 MHz," *Microw. Opt. Technol. Lett.*, vol. 57, no. 5, pp. 1125–1129, 2015.
[25] F. Wen and X. Huang, "Human exposure to electromagnetic fields from parallel wireless power transfer systems," *Int. J. Environ. Res. Public Health*, vol. 14, no. 2, p. 157, 2017.
[26] Q. Wang, W. Li, J. Kang, and Y. Wang, "Electromagnetic safety of magnetic resonant wireless charging system in electric vehicles," in *Proc. IEEE PELS Workshop Emerg. Technol., Wireless Power Transf. (WoW)*, May 2017, pp. 1–4.
[27] T. Nagaoka *et al.*, "Development of realistic high-resolution whole-body voxel models of Japanese adult males and females of average height and weight, and application of models to radio-frequency electromagnetic-field dosimetry," *Phys. Med. Biol.*, vol. 49, no. 1, pp. 1–15, 2004.
[28] A. Christ *et al.*, "The Virtual Family—Development of surface-based anatomical models of two adults and two children for dosimetric simulations," *Phys. Med. Biol.*, vol. 55, no. 2, p. N23, 2010.
[29] K. Aga, A. Hirata, and I. Laakso, "Intercomparison of In-situ electric field in human models for uniform magnetic field exposures," in *Proc. EMC Eur.*, Amsterdam, The Netherlands, 2018, pp. 515–520.
[30] S. Gabriel, R. W. Lau, and C. Gabriel, "The dielectric properties of biological tissues: III. Parametric models for the dielectric spectrum of tissues," *Phys. Med. Biol.*, vol. 41, no. 11, pp. 2271–2293, 1996.
[31] T. W. Dawson and M. A. Stuchly, "Analytic validation of a three-dimensional scalar-potential finite-difference code for low-frequency magnetic induction," *Appl. Comput. Electromagnet. J.*, vol. 11, no. 3, pp. 72–81, 1996.
[32] A. Hirata, F. Ito, and I. Laakso, "Confirmation of quasi-static approximation in SAR evaluation for a wireless power transfer system," *Phys. Med. Biol.*, vol. 58, no. 17, p. N241, 2013.
[33] R. Kavet, T. Dovan, and J. P. Reilly, "The relationship between anatomically correct electric and magnetic field dosimetry and published electric and magnetic field exposure limits," *Radiat. Protection Dosimetry*, vol. 152, no. 4, pp. 279–295, 2012.
[34] II Foundation. (May 17, 2018). *Database: Dielectric Properties*. [Online]. Available: https://www.itis.ethz.ch/virtual-population/tissue-properties/database/dielectric-properties/
[35] A. Barchanski, H. De Gersem, E. Gjonaj, and T. Weiland, "Impact of the displacement current on low-frequency electromagnetic fields computed using high-resolution anatomy models," *Phys. Med. Biol.*, vol. 50, no. 19, p. N243, 2005.
[36] N. Orcutt and O. P. Gandhi, "A 3-D impedance method to calculate power deposition in biological bodies subjected to time varying magnetic fields," *IEEE Trans. Biomed. Eng.*, vol. 35, no. 8, pp. 577–583, Aug. 1988.
[37] J. De Moerloose, T. W. Dawson, and M. A. Stuchly, "Application of the finite difference time domain algorithm to quasi-static field analysis," *Radio Sci.*, vol. 32, no. 2, pp. 329–341, 1997.
[38] S. Ilvonen and I. Laakso, "Computational estimation of magnetically induced electric fields in a rotating head," *Phys. Med. Biol.*, vol. 54, no. 2, p. 341, 2008.
[39] I. Laakso and A. Hirata, "Fast multigrid-based computation of the induced electric field for transcranial magnetic stimulation," *Phys. Med. Biol.*, vol. 57, no. 23, pp. 7753–7765, 2012.
[40] M. T. Jones and P. E. Plassmann, "An improved incomplete Cholesky factorization," *ACM Trans. Math. Softw.*, vol. 21, no. 1, pp. 5–17, 1995.
[41] R. Fletcher, "Conjugate gradient methods for indefinite systems," in *Numerical Analysis*. Berlin, Germany: Springer, 1976, pp. 73–89.
[42] G. L. G. Sleijpen and H. A. Van der Vorst, "A Jacobi–Davidson iteration method for linear eigenvalue problems," *SIAM Rev.*, vol. 42, no. 2, pp. 267–293, 2000.
[43] A. Hirata, Y. Takano, O. Fujiwara, T. Dovan, and R. Kavet, "An electric field induced in the retina and brain at threshold magnetic flux density causing magnetophosphenes," *Phys. Med. Biol.*, vol. 56, no. 13, pp. 4091–4101, 2011.
[44] A. Hirata, Y. Takano, Y. Kamimura, and O. Fujiwara, "Effect of the averaging volume and algorithm on the *in situ* electric field for uniform electric- and magnetic-field exposures," *Phys. Med. Biol.*, vol. 55, no. 9, pp. N243–N252, 2010.
[45] M. Soldati, M. Mikkonen, I. Laakso, T. Murakami, Y. Ugawa, and A. Hirata, "A multi-scale computational approach based on TMS experiments for the assessment of electro-stimulation thresholds of the brain at intermediate frequencies," *Phys. Med. Biol.*, vol. 63, no. 22, p. 225006, 2018.

KATSUAKI AGA received the B.E. degree in electrical and computer engineering from the National Institute of Technology, Kagawa College, Japan, in 2017. He is currently pursuing the master's degree in electrical and mechanical engineering with the Nagoya Institute of Technology, Nagoya, Japan.

His current research focuses on human protection from electromagnetic field at low and intermediate frequency.

AKIMASA HIRATA (S'98–M'01–SM'10–F'17) received the B.E., M.E., and Ph.D. degrees in communications engineering from Osaka University, Suita, Japan, in 1996, 1998, and 2000, respectively.

He was a Visiting Research Scientist with the University of Victoria, Victoria, BC, Canada, in 2000. In 2001, he joined the Department of Communications Engineering, Osaka University, as an Assistant Professor. In 2004, he joined the Department of Computer Science and Engineering, Nagoya Institute of Technology, as an Associate Professor, where he is currently a Full Professor. His research interests include electromagnetics and thermodynamics in biological tissue, waveguide analysis, electromagnetic compatibility and electromagnetic interference, and computational techniques in electromagnetics. From 1999 to 2001, he was a Research Fellow of the Japan Society for the Promotion of Science.

Dr. Hirata is a member of the IEICE, the IEE Japan, and the Bioelectromagnetics Society. He is a fellow of the Institute of Physics. He received several awards, including the Young Scientists' Prize in 2006, Prizes for Science and Technology (Research Category 2011 and Public Understanding Promotion Category 2014) by the Commendation for Science and Technology by the Minister of Education, Culture, Sports, Science, and Technology, Japan, the IEEE EMC-S Technical Achievement Award in 2015, and the Japan Academy Medal in 2018. He is an Editorial Board Member of physics in medicine and biology, a member of the Main Commission, the Chair of the Project Group of the International Commission on Non-Ionizing Radiation Protection, a member of the Administrative Committee, the Subcommittee (Electromagnetic Field Dosimetry Modeling) Chair of the IEEE International Committee on Electromagnetic Safety, and an expert of the World Health Organization. From 2006 to 2012, he was also an Associate Editor of the IEEE Transactions on Biomedical Engineering.

ILKKA LAAKSO (M'14) received the M.Sc. (Tech.) degree in electromagnetics from the Helsinki University of Technology, Espoo, Finland, in 2007, and the D.Sc. (Tech.) degree in electromagnetics from Aalto University, Espoo, in 2011.

From 2013 to 2015, he was a Research Assistant Professor and a Research Associate Professor with the Department of Computer Science and Engineering, Nagoya Institute of Technology. Since 2015, he has been an Assistant Professor in electromagnetics in health technologies with Aalto University. He has authored more than 80 papers published in international journals and conference proceedings. His current research focuses on computational bioelectromagnetic modeling for assessment of human safety and biomedical applications.

Dr. Laakso is a member of the Scientific Expert Group of the International Commission on Non-Ionizing Radiation Protection. He received several awards, including the Student Award from the International Symposium on Electromagnetic Compatibility, Kyoto, in 2009, the Ericsson Young Scientist Award in 2011, and the Young Scientist Award from the URSI General Assembly and Scientific Symposium, Montreal, Canada, in 2017. He is the Secretary and the Working Group Chair of the Subcommittee of Electromagnetic Field Dosimetry Modeling of the IEEE International Committee on Electromagnetic Safety.

HIROO TARAO was born in 1971. He received the B.S., M.S., and Ph.D. degrees in electrical engineering from the University of Tokushima, Japan, in 1994, 1996, and 1999, respectively. In 1999, he joined the Department of Electrical Engineering, Takamatsu National College of Technology, as an Assistant Professor. He is currently an Associate Professor with the Department of Electrical and Computer Engineering, National Institute of Technology, Kagawa College, Japan.

His current research interests are in electromagnetic environmental problems from power frequency to intermediate frequency, and the interaction of electromagnetic fields with biological systems. He is a member of the IEE Japan.

YINLIANG DIAO (M'17) received the B.E. degree from Chongqing University, Chongqing, China, in 2008, the M.S. degree in electronic engineering from the Beijing University of Posts and Telecommunications, Beijing, China, in 2011, and the Ph.D. degree in electronic engineering from the City University of Hong Kong, Hong Kong, in 2016. In 2017, he joined South China Agricultural University, Guangzhou, China, as an Assistant Professor.

His research interests include human safety issues in electromagnetic compatibility, and bioelectromagnetics.

TAKAHIRO ITO received the B.E., M.E., and Ph.D. degrees from the Nagoya Institute of Technology, Japan, in 2013, 2015, and 2017, respectively. Since 2017, he has been an Assistant Professor with the Graduate School of Engineering, Nagoya Institute of Technology. He is engaged in the research of computational electromagnetics in biology and medical applications.

YOICHI SEKIBA received the B.S. and M.S. degrees in physics from Tohoku University, Sendai, Japan, in 2008 and 2010, respectively. In 2010, he joined the Denryoku Computing Center, Tokyo, Japan. From 2013 to 2016, he was a Temporary Assignment Researcher with the Central Research Institute of Electric Power Industry, Yokosuka, Japan.

His current research focuses on the evaluation of human exposure to electromagnetic field by numerical electromotive force analysis. His research interests include the analysis of power systems by electromagnetic transient simulations. He is a member of the IEE Japan.

KENICHI YAMAZAKI (M'95–SM'06) was born in Yokohama, Japan, in 1968. He received the B.S. degree in applied physics from the Tokyo University of Science, Tokyo, Japan, in 1990, and the M.S. and Ph.D. degrees in biomedical engineering from Hokkaido University, Sapporo, Japan, in 1992 and 2001, respectively. In 1992, he joined the Central Research Institute of Electric Power Industry (CRIEPI), Tokyo. In 2002 and 2003, he was a Visiting Scientist with the School of Electrical Engineering and Computer Science, Washington State University, Pullman, WA, USA. He is currently a Deputy Associate Vice President and the Leader of the Lightning and Electromagnetic Environment Research Section, CRIEPI, Yokosuka, Japan. His research interests include the characterization of human exposure to low-frequency electromagnetic fields and power line electromagnetic compatibility. He is a member of the Bioelectromagnetics Society.